*Int. J. Solids Structures*, 1970, Vol. 6, pp. 91 to 116. Pergamon Press. Printed in Great Britain

# CREEP BUCKLING OF A CYLINDRICAL SHELL† UNDER NON-UNIFORM EXTERNAL LOADS

LARS ÅKE SAMUELSON‡

Lockheed Palo Alto Research Laboratories,
Palo Alto, California

**Abstract**—A method of analysis is presented for circular cylindrical shells under non-uniform external loads. The equations are valid for moderately large displacements and take secondary creep into account. Thermal effects and initial imperfections are included.

As the general equations are non-linear, an iterative method is used in the numerical analysis. The non-linear terms are at a certain iteration considered as known, generally determined by the previous iteration. They may thus be regarded as pseudo loads which are added to the actual external load terms. The variables of the thus linearized differential equations are expanded in Fourier series with respect to the circumferential coordinate. As a result, a series of sets of ordinary differential equations is obtained, one set for each Fourier index. These sets of equations are solved by use of a finite difference method. For each load or time step the equations are repeatedly solved until convergence is obtained.

A computer program was developed and was verified by comparison with known solutions for elastic buckling of shells. The theoretical behavior of a cylinder under creep is demonstrated for a number of different loading conditions, in particular the response is studied of an imperfect shell under uniform loads. In the case of external pressure, the critical time was found to be extremely sensitive to the imperfection shape. For a short cylinder under axial compression the presence of initial imperfections was shown to shorten the creep life substantially in comparison with the critical time corresponding to axisymmetrical collapse of the perfect shell.

## NOTATION

| | |
|---|---|
| $x, \varphi, z$ | Coordinates |
| $t$ | Time |
| $T$ | Temperature |
| $u, v, w$ | Displacements in the $x$, $\varphi$ and $z$ directions |
| $\varepsilon, \gamma$ | Strains |
| $\sigma, \tau$ | Stresses |
| $N$ | In-plane forces |
| $Q$ | Shear forces |
| $M$ | Bending moments |
| $p_x, p_\varphi, p_r$ | Body forces |
| | Defined in Figs. 2 and 3. |
| $N$ | Nonsubscripted, applied axial compressive load |
| $R$ | Radius of shell |
| $L$ | Length of shell |
| $h$ | Wall thickness |
| $b$ | Membrane distance in the idealized sandwich shell model, Fig. 1. |
| $E$ | Young's modulus |
| $\nu$ | Poisson's ratio |
| $B$ | Creep constant |
| $m$ | Creep exponent |
| $\eta$ | Coefficient of thermal expansion |
| $k, D, K$ | Stiffness coefficients defined by (8)–(10) |

† The present investigation was sponsored by the U.S. Navy under Contract No. NOOO 3066CO186. The author is greatly indebted to Mr. B. O. Almroth, of the Solid Mechanics Group for his advice and helpful criticism during the development of the theory and in preparing this report.

‡ Research Scientist, Sr., Aerospace Sciences Laboratory, presently at the Aeronautical Research Institute of Sweden (FFA).

| | |
|---|---|
| $H_1$–$H_6$ | Creep terms, equations (13) |
| **P**, **Q**, **R** | Right hand sides of equations (14) |
| $\Delta x$ | Step length in axial direction |
| $\Delta\varphi$ | Step length in circumferential direction used in the numerical evaluation of $H_1$–$H_6$ |
| $\Delta t$ | Step length in time |
| $n$ | Fourier coefficient number |
| $a_1$–$a_{29}$ | Coefficients of the finite difference equations (21) |
| $N_p$ | Number of "panels" in the circumferential direction |
| $N_F$ | Total number of Fourier terms to be used in the analysis |
| $N_x$ | Number of mesh points in the axial direction $L = \Delta x(N_x - 1)$ |
| $A_L$, $A_U$ | Limits determining the accuracy of the time integration |
| $e$ | Convergence criterion in the iteration procedure |
| $(\dot{f})$ | Denotes differentiation with respect to time or load. |
| $(f)'$ | Differentiation with respect to the axial coordinate $x$ |
| $(f)^{\cdot}$ | Differentiation with respect to the circumferential coordinate $\varphi$ |
| Dimensions: | In the specific examples below the dimensions of millimetres, kilograms and hours were used but, naturally, any dimensional system may be utilized. |

## INTRODUCTION

THE SOLUTION of the general shell equations is very complicated, particularly if non-symmetric loading is considered, and even for the case of elastic shells, solutions became available only recently. A first analysis was presented by Kalnins [1], who solved the linear equations for a shell of revolution under arbitrary loads. He separated the variables by expanding them into Fourier series with respect to the circumferential coordinate and thus obtained a series of uncoupled ordinary differential equations. These were solved by use of a numerical method. Such separation of the variables is however, in general, possible only in the linear case.

In a recent report, Ball [2], treated the same problem, but, in addition, the geometrically non-linear terms were included in the analysis. The equations were solved in a way similar to that by Kalnins. The effect of the non-linear terms was taken into account by use of an iterative method. As non-linear effects were included, the analysis can predict the collapse loads of the shell.

A third approach to the problem of shells of revolution under arbitrary loads was presented by Stricklin, *et al.* [3] who used a finite element method to calculate deformations and stresses.

The problem of creep in shell structures has attracted an increasing interest in recent years. So far, however, the attempts to solve the problems theoretically have been limited to special cases such as axial symmetry [4–10]. In most of these attempts, the deformations have been calculated in a direct way as functions of time [4–9], while in [10] the results in plastic buckling of shells were extended to the creep case by use of isocronous stress–strain curves.

A first attempt to analyze the creep behavior of a cylindrical shell under arbitrary loads was made in [11] and the present work is a continuation of that effort.

The governing equations for a circular cylindrical shell subjected to secondary creep are derived. The general procedure of [12] is followed. Non-linear terms are retained in the analysis and the effect of non-uniform temperature distributions and initial imperfections are included. The method of solution of the general set of non-linear partial differential equations is similar to that by Ball [2]. The non-linear effects are taken into account through an iterative procedure in which the non-linear terms at a certain iteration step are determined from the solution obtained in the previous step, or, for the very first step, from

the linear solution. The non-linear terms may then be added to the external load terms and can thus be regarded as pseudo loads. By expansion of the deflection and the load terms into Fourier series with respect to the circumferential coordinate, a series of sets of ordinary differential equations is obtained, one set for each Fourier index. As these sets are derived from the "linearized" general equations, in which the non-linear terms are regarded as pseudo loads, they can be solved independently of each other. The coupling, which does exist between the different sets of equations is accounted for through iteration.

The loads of the elastic shell are applied in small steps and the integration in time in the presence of creep is carried out by use of small time steps. For each incremental load or time step, the non-linear terms from the solution at the previous step are used as a first estimate. An iterative procedure is then applied until convergence is obtained.

## ASSUMPTIONS

The following assumptions are made:

1. The material is characterized by linear elasticity according to Hooke and secondary creep governed by the power law.
2. The shell wall can be replaced by a double membrane model, Fig. 1; this is commonly done in problems where creep is involved.
3. Normals to the undeformed middle surface remain straight and normal during the deformation of the shell.
4. Terms representing geometrical non-linearities are included in the kinematics relations and in the equations of equilibrium according to the Donnell approximation.
5. Radial stresses are negligible.

## THEORY

The derivation of the governing differential equations was done along the lines of Ref. [12], Chapter 5. However, second order terms are retained in the equations of equilibrium and kinematics and a secondary creep strain component is introduced in the relation for the material behavior.

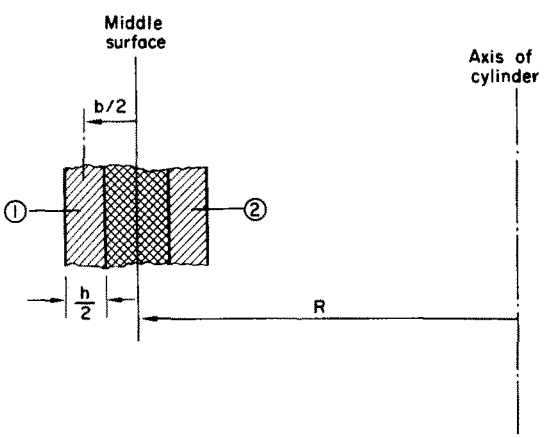


FIG. 1. Definition of the double membrane model.

*Material properties*

The material is assumed to be isotropic, the elastic part of the stress–strain relation being governed by Hooke's law. Furthermore, the creep law is required to be of the form:

$$\dot{\varepsilon} = \frac{\dot{\sigma}}{E} + B\sigma^m + \eta\dot{T}. \tag{1}$$

The extension of (1) to the case of two-dimensional stress can be written as:

$$\begin{cases} \dot{\varepsilon}_x = \dfrac{1}{E}(\dot{\sigma}_x - \nu\dot{\sigma}_\varphi) + B(3I)^{(m-1)/2}(\sigma_x - \tfrac{1}{2}\sigma_\varphi) + \eta\dot{T} \\ \dot{\varepsilon}_\varphi = \dfrac{1}{E}(\dot{\sigma}_\varphi - \nu\dot{\sigma}_x) + B(3I)^{(m-1)/2}(\sigma_\varphi - \tfrac{1}{2}\sigma_x) + \eta\dot{T} \\ \dot{\gamma}_{x\varphi} = \dfrac{2(1+\nu)}{E}\dot{\tau}_{x\varphi} + 3B(3I)^{(m-1)/2}\tau_{x\varphi} \end{cases} \tag{2}$$

where the stress invariant $I$ is defined by

$$I = \sigma_e^2 = \tfrac{1}{3}(\sigma_x^2 + \sigma_\varphi^2 - \sigma_x\sigma_\varphi + 3\tau_{x\varphi}^2). \tag{3}$$

*Equilibrium*

The internal and external forces and moments acting on a shell element are defined in Figs. 2 and 3. The conditions of equilibrium yield the following four equations:

$$\begin{cases} RN'_x + N^{\cdot}_{\varphi x} = -p_x R \\ RN^{\cdot}_\varphi + R^2 N'_{x\varphi} - M^{\cdot}_\varphi - RM'_{x\varphi} = -p_\varphi R^2 \\ M^{\cdot\cdot}_\varphi + RM^{\cdot\cdot}_{x\varphi} + RM^{\cdot\cdot}_{\varphi x} + R^2 M''_x + RN_\varphi = (N_\varphi w^{\cdot} + RN_{x\varphi}w')^{\cdot} + (R^2 N_x w' + RN_{x\varphi}w^{\cdot})' + p_r R^2 \\ RN_{x\varphi} - RN_{\varphi x} + M_{\varphi x} = 0. \end{cases} \tag{4}$$

Here the shear forces have been eliminated. The linear terms of these equations are identical to those by Flügge [11].

*Sandwich shell model*

The sandwich shell model is utilized in the analysis. It was shown in [9] that if the distance between the two membranes is chosen such that the bending stiffness of the

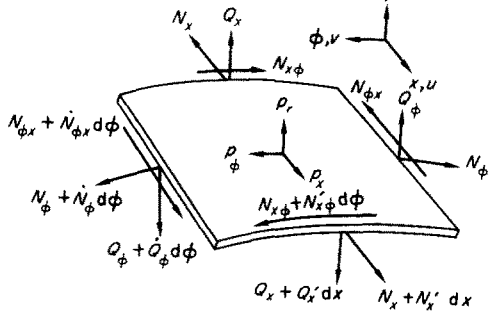


FIG. 2. Definition of the internal forces.

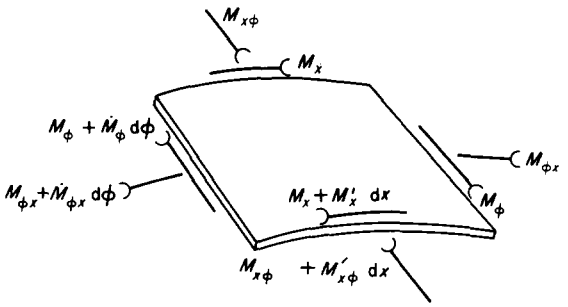


FIG. 3. Definition of internal moments.

model is the same as that of the real shell, use of this model leads to an estimate of the critical time in creep buckling which is very close to that obtained with more accurate multi-membrane models. Hence it is assumed that, see Fig. 1:

$$b = h/\sqrt{3}. \tag{5}$$

*Deformations*

According to Flügge [12], pp. 212 and 469, the strains are related to the displacements in the following way:

$$\begin{cases} \varepsilon_x = u' - zw'' + \frac{1}{2}w'^2 \\ \varepsilon_\varphi = \dfrac{1}{R}\dot{v} - \dfrac{z}{R}\dfrac{\ddot{w}}{R+z} + \dfrac{w}{R+z} + \dfrac{1}{2R^2}\dot{w}^2 \\ \gamma_{x\varphi} = \dfrac{\dot{u}}{R+z} + \dfrac{R+z}{R}v' - \left(\dfrac{z}{R} + \dfrac{z}{R+z}\right)\dot{w}' + \dfrac{1}{R}w'\dot{w}. \end{cases} \tag{6}$$

In the sandwich model the strains are represented by the values at the midpoint of each layer, that is $z_1 = b/2$ and $z_2 = -b/2$, where $z_1$ and $z_2$ are the $z$ coordinates of the outer and inner membranes respectively. Insertion of these values and rearrangement of the equations yield the following strain–displacement relations

$$\begin{cases} \varepsilon_{x1} - \varepsilon_{x2} = -bw'' \\ \varepsilon_{x1} + \varepsilon_{x2} = 2u' + w'^2 \\ \varepsilon_{\varphi 1} - \varepsilon_{\varphi 2} = -\dfrac{4}{b}k\dot{w}' - \dfrac{4}{b}kw \\ \varepsilon_{\varphi 1} + \varepsilon_{\varphi 2} = \dfrac{2}{R}\dot{v} + \dfrac{2}{R}k\dot{w}' + \dfrac{2}{R}w + \dfrac{1}{R^2}\dot{w}^2 \\ \gamma_{x\varphi 1} - \gamma_{x\varphi 2} = -\dfrac{4}{b}k\dot{u} + \dfrac{b}{R}v' - \dfrac{2b}{R}\dot{w}' \\ \gamma_{x\varphi 1} + \gamma_{x\varphi 2} = \dfrac{2}{R}\dot{u} + 2v' + 2k\dot{w}' + \dfrac{2}{R}w'\dot{w}. \end{cases} \tag{7}$$

*Assembling the equations*

The following notations will be used below:

$$D = Eh/(1-\nu^2) \tag{8}$$

$$K = Eh^3/12(1-\nu^2)\ . \tag{9}$$

$$k = \frac{K}{DR^2} = \frac{h^2}{12R^2} = \frac{b^2}{4R^2}. \tag{10}$$

The relations between forces and bending moments and stresses are:

$$\begin{cases}
N_x = \int_{-h/2}^{h/2} \sigma_x\left(1+\frac{z}{R}\right) dz = \frac{h}{2}[\sigma_{x1}(1+\sqrt{k})+\sigma_{x2}(1-\sqrt{k})] \\
N_\varphi = \int_{-h/2}^{h/2} \sigma_\varphi\, dz = \frac{h}{2}[\sigma_{\varphi 1}+\sigma_{\varphi 2}] \\
N_{x\varphi} = \int_{-h/2}^{h/2} \tau_{x\varphi}\left(1+\frac{z}{R}\right) dz = \frac{h}{2}[\tau_{x\varphi 1}(1+\sqrt{k})+\tau_{x\varphi 2}(1-\sqrt{k})] \\
N_{\varphi x} = \int_{-h/2}^{h/2} \tau_{\varphi x} dz = \frac{h}{2}[\tau_{x\varphi 1}+\tau_{x\varphi 2}] \\
M_x = -\int_{-h/2}^{h/2} \sigma_x\left(1+\frac{z}{R}\right) z\, dz = -\frac{hb}{4}[\sigma_{x1}(1+\sqrt{k})-\sigma_{x2}(1-\sqrt{k})] \\
M_\varphi = -\int_{-h/2}^{h/2} \sigma_\varphi z\, dz = -\frac{hb}{4}[\sigma_{\varphi 1}-\sigma_{\varphi 2}] \\
M_{x\varphi} = -\int_{-h/2}^{h/2} \tau_{x\varphi}\left(1+\frac{z}{R}\right) z\, dz = -\frac{hb}{4}[\tau_{x\varphi 1}(1+\sqrt{k})-\tau_{x\varphi 2}(1-\sqrt{k})] \\
M_{\varphi x} = -\int_{-h/2}^{h/2} \tau_{\varphi x} z\, dz = -\frac{hb}{4}[\tau_{x\varphi 1}-\tau_{x\varphi 2}].
\end{cases} \tag{11}$$

The relations above define the complete set of governing equations for a circular cylindrical shell. It is convenient to work with a set of equations in terms of the deformation components $u$, $v$ and $w$. Therefore, the strain rates, given by (2), are inserted in the kinematic expression (7). The result is a set of six equations for the unknown stress rates $\dot\sigma_{x1}-\dot\tau_{x\varphi 2}$, which, after reduction, yields:

$$\begin{cases}
\dot\sigma_{x1} = \frac{E}{2(1-\nu^2)}\Big[2\dot u' + \frac{2\nu}{R}\dot v^{\cdot} - b\dot w'' - \frac{4\nu}{b}k\dot w^{\cdot\cdot} + \frac{2\nu}{R}(1-\sqrt{k})\dot w \\
\qquad\qquad + \frac{\partial}{\partial t}w'^2 + \frac{\nu}{R^2}\frac{\partial}{\partial t}w^{\cdot 2} + H_1 + H_2 + \nu(H_3+H_4)\Big] \\
\dot\sigma_{x2} = \frac{E}{2(1-\nu^2)}\Big[2\dot u' + \frac{2\nu}{R}\dot v^{\cdot} + b\dot w'' + \frac{4\nu}{b}k\dot w^{\cdot\cdot} + \frac{2\nu}{R}(1+\sqrt{k})\dot w \\
\qquad\qquad + \frac{\partial}{\partial t}w'^2 + \frac{\nu}{R^2}\frac{\partial}{\partial t}w^{\cdot 2} - H_1 + H_2 - \nu(H_3-H_4)\Big]
\end{cases} \tag{12}$$

$$
\begin{aligned}
\dot{\sigma}_{\varphi 1} &= \frac{E}{2(1-\nu^2)}\Big[2\nu\dot{u}' + \frac{2}{R}\dot{v}^{\cdot} - b\nu\dot{w}'' - \frac{4}{b}k\dot{w}^{\cdot\cdot} + \frac{2}{R}(1-\sqrt{k})\dot{w} \\
&\qquad + \nu\frac{\partial}{\partial t}w'^2 + \frac{1}{R^2}\frac{\partial}{\partial t}w^{\cdot 2} + \nu(H_1+H_2) + H_3 + H_4\Big] \\
\dot{\sigma}_{\varphi 2} &= \frac{E}{2(1-\nu^2)}\Big[2\nu\dot{u}' + \frac{2}{R}\dot{v}^{\cdot} + b\nu\dot{w}'' + \frac{4}{b}k\dot{w}^{\cdot\cdot} + \frac{2}{R}(1+\sqrt{k})\dot{w} \\
&\qquad + \nu\frac{\partial}{\partial t}w'^2 + \frac{1}{R^2}\frac{\partial}{\partial t}w^{\cdot 2} - \nu(H_1-H_2) - H_3 + H_4\Big] \\
\dot{t}_{x\varphi 1} &= \frac{E}{4(1+\nu)}\Big[\frac{2}{R}(1-\sqrt{k})\dot{u}^{\cdot} + 2(1+\sqrt{k})\dot{v}' - 2\sqrt{k}(2-\sqrt{k})\dot{w}^{\cdot} \\
&\qquad + \frac{2}{R}\frac{\partial}{\partial t}(w'w^{\cdot}) + H_5 + H_6\Big] \\
\dot{t}_{x\varphi 2} &= \frac{E}{4(1+\nu)}\Big[\frac{2}{R}(1+\sqrt{k})\dot{u}^{\cdot} + 2(1-\sqrt{k})\dot{v}' + 2\sqrt{k}(2+\sqrt{k})\dot{w}^{\cdot} \\
&\qquad + \frac{2}{R}\frac{\partial}{\partial t}(w'w^{\cdot}) - H_5 + H_6\Big].
\end{aligned}
\tag{12 contd.}
$$

Here the "creep terms" $H_1$–$H_6$ are defined as:

$$
\begin{aligned}
H_{1,2} &= -[B(3I_1)^{(m-1)/2}(\sigma_{x1} - \tfrac{1}{2}\sigma_{\varphi 1}) \mp B(3I_2)^{(m-1)/2}(\sigma_{x2} - \tfrac{1}{2}\sigma_{\varphi 2}) + \eta\dot{T}_1 \mp \eta\dot{T}_2] \\
H_{3,4} &= -[B(3I_1)^{(m-1)/2}(\sigma_{\varphi 1} - \tfrac{1}{2}\sigma_{x1}) \mp B(3I_2)^{(m-1)/2}(\sigma_{\varphi 2} - \tfrac{1}{2}\sigma_{x2}) + \eta\dot{T}_1 \mp \eta\dot{T}_2] \\
H_{5,6} &= -3B[(3I_1)^{(m-1)/2}\tau_{x\varphi 1} \mp (3I_2)^{(m-1)/2}\tau_{x\varphi 2}].
\end{aligned}
\tag{13}
$$

By combination of (11), (12) and the equilibrium equations (4), the governing equations are finally expressed in terms of the deflection rates $\dot{u}$, $\dot{v}$ and $\dot{w}$:

$$
\begin{aligned}
&R^2\dot{u}'' + \frac{1-\nu}{2}\dot{u}^{\cdot\cdot} + R\frac{1+\nu}{2}\dot{v}^{\cdot\cdot} + R\nu\dot{w}' + k\left(\frac{1-\nu}{2}\dot{u}^{\cdot\cdot} - R^3\dot{w}''' + R\frac{1-\nu}{2}\dot{w}^{\cdot\cdot\cdot}\right) \\
&\quad = -\frac{R^2}{D}\dot{p}_x - R^2\frac{\partial}{\partial t}(w'w'') - \nu\frac{\partial}{\partial t}(w^{\cdot}w^{\cdot\cdot}) - \frac{1}{2}(1-\nu)\frac{\partial}{\partial t}(w'w^{\cdot\cdot} + w^{\cdot\cdot}w^{\cdot}) \\
&\qquad -\frac{R^2}{2}[H_2' + \nu H_4' + \sqrt{k}(H_1' + \nu H_3')] + R\frac{1-\nu}{4}H_6^{\cdot} = \mathbf{P} \\
&R\frac{1+\nu}{2}\dot{u}^{\cdot\cdot} + \dot{v}^{\cdot\cdot} + R^2\frac{1-\nu}{2}\dot{v}'' + \dot{w}^{\cdot} + k\left(\frac{3(1-\nu)}{2}R^2\dot{v}'' - \frac{3-\nu}{2}R^2\dot{w}^{\cdot\cdot}\right) \\
&\quad = -\frac{R^2}{D}\dot{p}_{\varphi} - R\frac{1+\nu}{2}\frac{\partial}{\partial t}(w'w^{\cdot}) - R\frac{1-\nu}{2}\frac{\partial}{\partial t}(w''w^{\cdot}) - \frac{1}{R}\frac{\partial}{\partial t}(w^{\cdot}w^{\cdot\cdot}) \\
&\qquad -\frac{R}{2}[\nu H_2^{\cdot} + H_4^{\cdot} + \sqrt{k}(\nu H_1^{\cdot} + H_3^{\cdot})] + \frac{R^2(1-\nu)}{4}[2\sqrt{k}H_5' + (1+k)H_6'] = \mathbf{Q}
\end{aligned}
\tag{14}
$$

$$
\begin{aligned}
&Rv\dot{u}' + \ddot{v} + \dot{w} + k\left(\frac{1-v}{2}R\dot{u}''' - R^3\dot{u}''' - \frac{3-v}{2}R^2\dot{v}''' + R^4\dot{w}^{IV} + 2R^2\dot{w}''''' + \ddot{w}'' + 2\dot{w}'' + \dot{w}\right) \\
&\quad = \frac{R^2}{D}\dot{p}_r + R\frac{1-v}{2}k\frac{\partial}{\partial t}(w'w''' + w'^2 + w''w'' + w'''w') + R^3k\frac{\partial}{\partial t}(w''^2 + w'w''') \qquad \text{(14 contd.)} \\
&\quad + vRk\frac{\partial}{\partial t}(\dot{w}'w''' + \dot{w}'^2) - \frac{1}{2}Rv\frac{\partial}{\partial t}(w'^2) - \frac{1}{2R}\frac{\partial}{\partial t}(w'^2) \\
&\quad + \frac{1}{2}R^3\sqrt{k}[H_1'' + vH_3'' + \sqrt{k}(H_2'' + vH_4'')] + \frac{R}{2}\sqrt{k}[vH_1'' + H_3''] \\
&\quad - \frac{R}{2}[vH_2 + H_4] + \frac{R^2}{4}(1-v)\sqrt{k}[2H_5'' + \sqrt{k}H_6''] \\
&\quad + \frac{1}{D}\frac{\partial}{\partial t}[(N_\varphi w' + RN_{x\varphi}w')' + (R^2N_x w' + RN_{x\varphi}w')' = \mathbf{R}.
\end{aligned}
$$

The fourth of Equations (4) is identically satisfied due to the fact that $\tau_{x\varphi} = \tau_{\varphi x}$. The linear part of equations (14) is identical with Flügge's (Ref. [12], equations (13), p. 219).

*Boundary conditions*

Four different sets of boundary conditions were considered in the investigation.

*Case C1. Simple support.*

$$
\begin{cases}
x = 0: \\
u = v = w = M_x = 0 \\
x = L: \\
v = w = M_x = 0 \\
-\int_0^{2\pi} N_x R\, d\varphi = N.
\end{cases} \qquad (15)
$$

*Case C2. Classical simple support.* In this case an axial force is assumed uniformly distributed around the circumference.

$$
\begin{cases}
x = 0: \\
v = w = M_x = 0 \\
N_x = -N/2\pi R \\
x = L: \\
v = w = M_x = 0 \\
N_x = -N/2\pi R.
\end{cases} \qquad (16)
$$

*Case C3. Clamped edges.*

$$\begin{cases} x = 0: \\ u = v = w = w' = 0 \\ x = L: \\ v = w = w' = 0 \\ -\int_0^{2\pi} N_x R \, d\varphi = N. \end{cases} \tag{17}$$

*Case C.4. Laterally unrestrained edges.* In the study of a long cylinder with local imperfections and subjected to uniform axial compression or external pressure, the following procedure may be applied: Assume that the imperfections are of equal form and amplitude and are uniformly distributed along the axial and circumferential coordinates. Then the small portions of the cylinder surrounding each imperfection may be analyzed separately if the conditions of symmetry are applied at the boundaries. If the imperfections are very localized the following equations are obtained.

$$\begin{cases} x = 0: \\ u = v = w' = 0 \\ w = f(N, p_r, t) \\ x = L: \\ v = w' = 0 \\ w = f(N, p_r, t) \\ -\int_0^{2\pi} N_x R \, d\varphi = N. \end{cases} \tag{18}$$

*Initial imperfections*

Initial imperfections play an extremely important rôle in certain cases of uniform loading of cylindrical shells. It is therefore important that the effect of initial defects is included in the analysis.

In the following, it will be assumed that the shell has an initial radial displacement $w_0$ which is a function of the spatial coordinates. In the equilibrium equations (4) the displacement $w$ represents the total displacement and these equations are thus still valid. On the other hand, it is assumed that the shell is stress-free in the unloaded state which means that the strains given by (6) must vanish. As the total deflection $w$ in the unloaded state is equal to the initial imperfection $w_0$, it is clear that $w$ in the linear part of (6) must be replaced by $(w - w_0)$. Simple geometrical considerations also imply that the non-linear terms are replaced by for instance $\frac{1}{2}(w'^2 - w_0'^2)$.

The final equations (12) and (14) were derived by use of (6) through differentiation with respect to time. As $\dot{w}_0 = 0$, the final equations are thus valid in their original form where it is assumed that $w = w_0$ for zero load.

*Method of solution*

In the general equations (14), the non-linear terms and the creep terms were placed on the right-hand side of the equality sign together with the load terms. It is assumed that at a certain iteration, the solution at the previous step or the previous iteration cycle is available. This solution is used to estimate the values of the non-linear terms at the current iteration. The equations are solved repeatedly until convergence is obtained. The expression defined by the symbol **P** in (14) may be written as:

$$\mathbf{P} = -\frac{R^2}{D}\dot{p}_x + \dot{T}_{NL} + H_C \tag{19}$$

where $\dot{T}_{NL}$ represents all the geometrically non-linear terms and $H_C$ contains all terms involving the creep functions $H_1$–$H_6$. It is assumed that the right-hand sides of the general partial differential equations may be expanded into Fourier series:

$$\begin{cases} \mathbf{P} = \mathbf{P}_0 + \sum_{n=1}^{N_F} \mathbf{P}_n \cos n N_P \varphi \\ \mathbf{Q} = \sum_{n=1}^{N_F} \mathbf{Q}_n \sin n N_P \varphi \\ \mathbf{R} = \mathbf{R}_0 + \sum_{n=1}^{N_F} \mathbf{R}_n \cos n N_P \varphi. \end{cases} \tag{20}$$

Here the expansions for the external load terms $\dot{p}_{x_n}$ are given for the case to be analyzed. The evaluation of the pseudo load terms $\dot{T}_{NL_n}$ involves an expansion of the product of two Fourier series into a new series. This evaluation is done analytically as shown in Appendix A. The creep terms $H_{C_n}$ are functions of the stresses taken to the $m$th power, where $m$ is the creep exponent. These functions can be evaluated analytically only for odd integer values of $m$. As $m$ is in general a non-integer, a numerical integration scheme was used in the evaluation of the Fourier terms of the creep functions. See Appendix B.

The solution of equations (14) is represented by:

$$\begin{cases} \dot{u}(x, \varphi) = \dot{u}_0(x) + \sum_{n=1}^{N_F} \dot{u}_n(x) \cos n N_P \varphi \\ \dot{v}(x, \varphi) = \dot{v}_0(x) + \sum_{n=1}^{N_F} \dot{v}_n(x) \sin n N_P \varphi \\ \dot{w}(x, \varphi) = \dot{w}_0(x) + \sum_{n=1}^{N_F} \dot{w}_n(x) \cos n N_P \varphi. \end{cases} \tag{21}$$

By insertion of (20) and (21) in the general partial equations (14), which were "linearized" by regarding the non-linear terms as pseudo loads, a series of sets of ordinary differential equations is obtained, one for each Fourier index $n$. The solution of these equation systems is obtained by use of a finite difference method. Application of the commonly used central

difference expressions leads to the following form for the general equations:

$$\begin{cases} a_1\dot{w}_{\mu-2}+a_2\dot{u}_{\mu-1}+a_3\dot{v}_{\mu-1}+a_4\dot{w}_{\mu-1}+a_5\dot{u}_{\mu}+a_6\dot{u}_{\mu+1}+a_7\dot{v}_{\mu+1}+a_8\dot{w}_{\mu+1}+a_9\dot{w}_{\mu+2}=\mathbf{P}_{\mu} \\ a_{10}\dot{u}_{\mu-1}+a_{11}\dot{v}_{\mu-1}+a_{12}\dot{w}_{\mu-1}+a_{13}\dot{v}_{\mu}+a_{14}\dot{w}_{\mu}+a_{15}\dot{u}_{\mu+1}+a_{16}\dot{v}_{\mu+1}+a_{17}\dot{w}_{\mu+1}=\mathbf{Q}_{\mu} \\ a_{18}\dot{u}_{\mu-2}+a_{19}\dot{w}_{\mu-2}+a_{20}\dot{u}_{\mu-1}+a_{21}\dot{v}_{\mu-1}+a_{22}\dot{w}_{\mu-1}+a_{23}\dot{v}_{\mu}+a_{24}\dot{w}_{\mu}+a_{25}\dot{u}_{\mu+1} \\ \quad +a_{26}\dot{v}_{\mu+1}+a_{27}\dot{w}_{\mu+1}+a_{28}\dot{u}_{\mu+2}+a_{29}\dot{w}_{\mu+2}=\mathbf{R}_{\mu}. \end{cases} \tag{22}$$

There is one set of these equations for each Fourier index $n$ at each interior mesh point $\mu$. The boundary conditions provide eight additional conditions for each Fourier index. These conditions apply for the mesh points at the edges, $\mu = 1$ and $\mu = N_x$ and also modify the general equations (22) at the neighboring points $\mu = 2$ and $\mu = N_x - 1$. As an example, the boundary conditions corresponding to case C3, equations (17) at the edge $x = 0$ give:

$$\begin{cases} x = 0 \Rightarrow \\ \dot{u}_1 = 0 \\ \dot{v}_1 = 0 \\ \dot{w}_1 = 0 \\ \left.\begin{array}{l} a_4 \to a_4 - 1{\cdot}5a_1 \\ \bar{a}_5 = 3a_1 \text{ (coefficient of } \dot{w}_2) \\ a_8 = a_8 - 0{\cdot}5a_1 \\ a_{22} \to a_{22} - 1{\cdot}5a_{19} \\ a_{24} \to a_{24} + 3a_{19} \\ a_{27} \to a_{27} - 0{\cdot}5a_{19} \end{array}\right\} \text{Changes in the coefficients of the general equations at point } \mu = 2. \end{cases} \tag{23}$$

Equations (21) form, together with the appropriate boundary conditions, a set of algebraic equations with a strongly banded matrix as shown in Fig. 4, one set for each Fourier index.

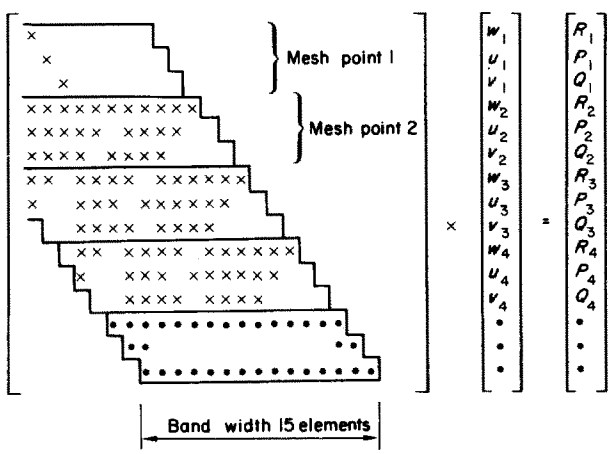


FIG. 4. Matrix of coefficients in the system of algebraic equations for the deflection rates $\dot{u}$, $\dot{v}$ and $\dot{w}$.

These equations are conveniently solved by means of Gaussian elimination and as the coefficients $a_i$ in (22) do not change from one iteration to another, this elimination need be done once only for a given case. The method used is described in [13]. The factored matrices are stored throughout the computations and are used to operate on the successively changing right-hand sides.

*Flow of calculations*

The general equations (14) are valid for the analysis of stresses and deformations in a cylinder subjected to creep. However, if the creep terms $H_i$ are disregarded and $(\dot{})$ is interpreted as differentiation with respect to some loading parameter $\bar{p}$, the equations are valid for an elastic shell subjected to changing external loads.

The computer program developed for the numerical analysis [13] can handle problems involving any number of load changes separated or followed by creep periods during which the external loads are constant. In general, it is possible to treat problems of creep under continuously varying loads, but it was shown in [14] that such a procedure is not economical because it requires a very small time step. It is therefore preferable to approximate the load history by a step function.

The analysis is carried out along the following lines: First the general input data are read into the program, together with initial imperfections, if such are included. Then the load changes are read in and the initial load step is prescribed. The incremental deflections and stresses are computed for each incremental load step by application of an iterative procedure. The first approximation is provided by the solution obtained in the previous load step or, for the first load step in each loading sequence, by the linear solution. A convergence criterion is applied to each Fourier coefficient at some fixed meridional coordinate. It is required that

$$\left| \left| \frac{\dot{w}^{\nu+1}}{\dot{w}^{\nu}} \right| - 1 \right| < e \tag{24}$$

where $e$ is an input parameter.

In the creep case it is necessary to choose a sufficiently small time step in order to ensure an adequate accuracy. On the other hand, a too small time step leads to higher computer times and therefore a condition similar to the convergence criterion (23) was adopted:

$$A_L < \left| \left| \frac{\dot{w}^{\nu+1}}{\dot{w}^{\nu}} \right| - 1 \right| < A_u. \tag{25}$$

If this condition is not satisfied, the time step is multiplied by either a factor of $\frac{1}{2}$ or 2, depending on whether the ratio is bigger than $A_u$ or less than $A_L$. Suitable values of $e$, $A_L$ and $A_u$ were determined by repeated computations with successively modified values of these parameters. An adequate accuracy for most purposes was obtained with $e$ and $A_L \sim 0{\cdot}01$–$0{\cdot}02$ and $A_u \sim 0{\cdot}02$–$0{\cdot}05$.

## RESULTS

A limited numerical analysis has been performed which demonstrates the applicability of the program.

*Collapse of elastic shells.*

In the classical theory of cylindrical shells subjected to uniform pressures, the buckling load is obtained through solution of an eigenvalue problem. However, it is well known that experimentally determined buckling pressures are always lower than the classical load. This is due to the fact that shells are sensitive to initial defects, which are always present in a real shell, and the classical theory was developed for perfect shells. The load–deflection characteristic of a cylindrical shell under axial compression is shown in Fig. 5a. With increasing load, the amplitudes of the deformations caused by an initial imperfection will grow until collapse occurs and the buckling load is extremely sensitive to the amplitude of the imperfection. This behavior is different from that of an elastic column, Fig. 5b, for which the buckling load $P$ is independent of the initial imperfection.

As the present analysis takes initial defects into consideration, it can be used for calculation of collapse loads. In particular, the buckling load obtained should agree with the classical solution independently of the shape and size of the imperfections, provided these are sufficiently small. A small deviation from uniformity of the external pressure would

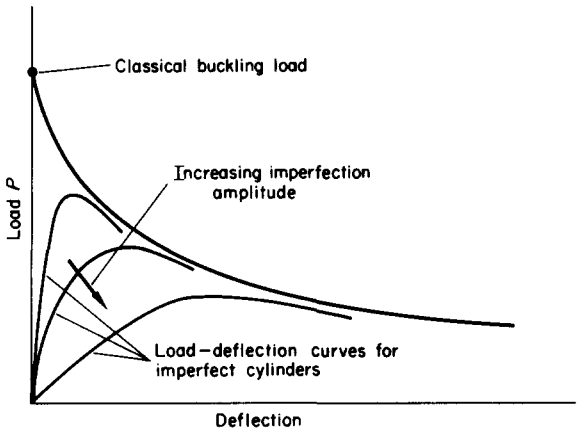


FIG. 5a. Load–deflection characteristic of an imperfect cylinder.

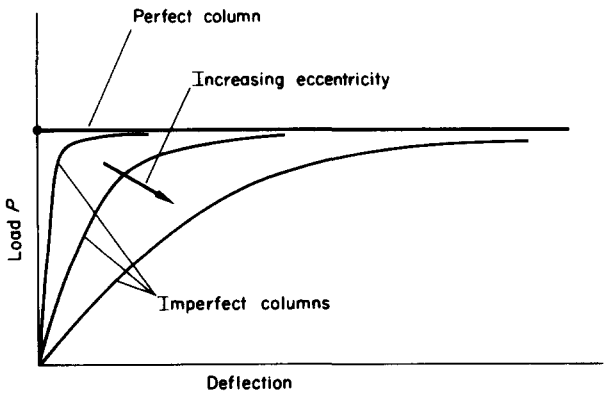


FIG. 5b. Load–deflection characteristic of an imperfect column.

have the same effect as an initial imperfection. For verification of the method of analysis, such an example was analyzed. The collapse pressure was calculated for a cylinder with $R/h = 100, L/R = 1$ and $E = 5000$. According to the classical buckling theory [11] buckling occurs into 8 waves at a pressure of $p = -0{\cdot}051$. A small nonuniform pressure was first applied, given by

$$\Delta p = 0{\cdot}0006\,(\cos 2\varphi + \cos 4\varphi + \cos 6\varphi + \cos 8\varphi). \tag{26}$$

A uniform pressure was then applied step wise until large deflections were obtained for small changes in load, thus indicating that the collapse load was approached. The results of the calculations are demonstrated in Fig. 6 in the form of deflection amplitudes at the midpoint of the shell, $(x = L/2)$, as functions of the load. It appears that the 8th harmonic of the deformation function dominates and collapse occurs for a load slightly lower than the classical buckling load. This result should be expected since the cylinder under external pressure is imperfection sensitive, although not to the same extent as cylinders in axial compression.

It has been verified by additional test cases that the same behavior is obtained if initial non-symmetric imperfections are prescribed instead of a pressure disturbance. Furthermore, it has been found that if the amplitudes of the initial imperfections are decreased, within

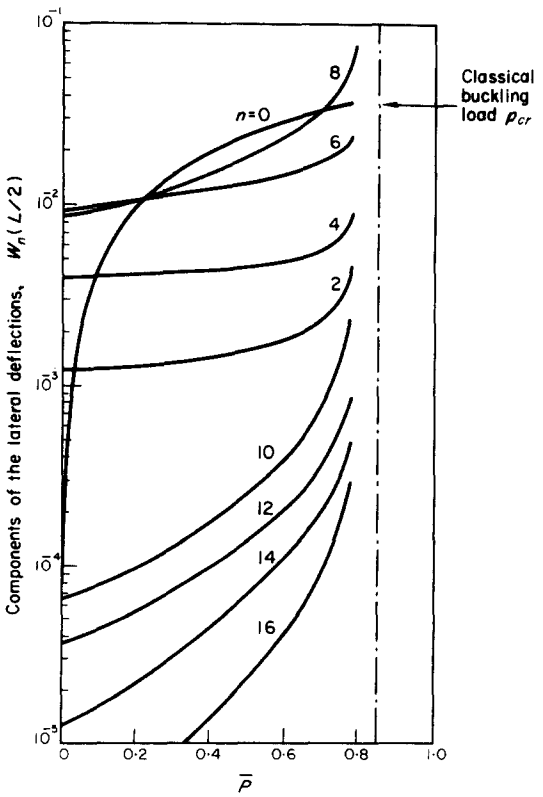


FIG. 6. Load–deflection curves for a cylinder with $R/h = 100$, $L/R = 1$ and $E = 5000$ subjected to radial pressure.

practical limits, the classical buckling load of the shell is approached. Severe imperfections on the other hand can lead to drastic reductions in the collapse load.

*Collapse under creep*

A cylindrical shell subjected to non-uniform external loads will, in the presence of creep, develop time dependent deformations and may eventually collapse. An example is given here which demonstrates the nature of the solution for a cylinder under circumferentially varying radial pressure:

(a) *Non-uniform external pressure.* A cylinder with $L/R = 5$, $R/h = 100$ and $E = 5000$ is subjected to a non-uniform radial pressure of the form:

$$p_r = -0{\cdot}001 \cos 2\varphi. \tag{27}$$

Under uniform external pressure, this cylinder buckles at $p_0 = -0{\cdot}0093$ according to the classical theory. The creep response to the nonsymmetrical load is demonstrated in Fig. 7.

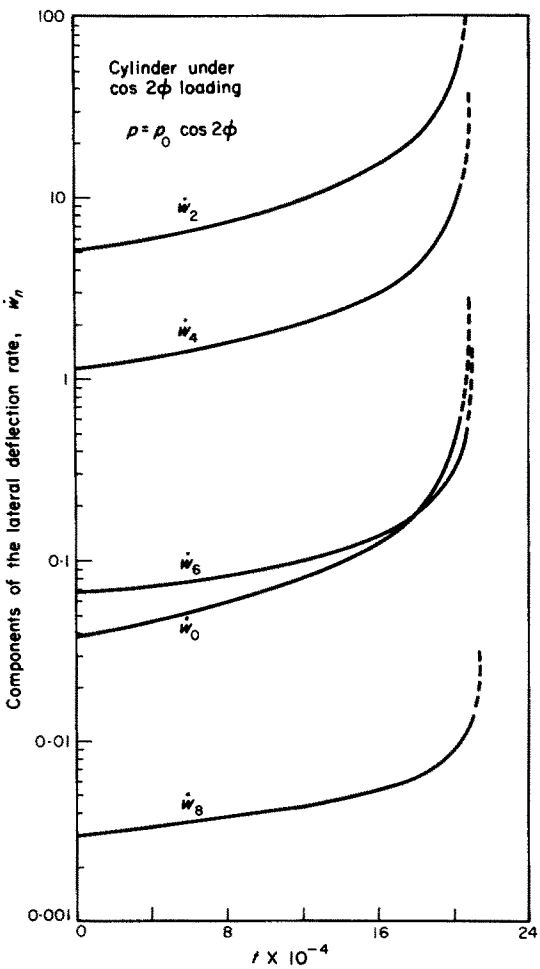


FIG. 7. Deflection–rate history of a cylinder under non-uniform external pressure. $R/h = 100$, $L/R = 5$, $E = 5000$ and $n = 5{\cdot}8$.

The amplitudes $\dot{w}_n$ in the Fourier expansion for the radial deflection rate $\dot{w}$ at the mid-point of the shell are shown as functions of time. It may be noted that although the applied load contains only the second harmonic, equation (27), displacements occur in higher harmonics as well. These are, however, quite small and collapse occurs into 2 waves. It is interesting to notice that although the deflection rates are large at the time $t = 19{\cdot}5 \times 10^{-4}$, see Fig. 7, the total deflections are still very small. For an outside observer, collapse would therefore seem to occur nearly instantaneously.

(b) *Uniform radial pressure, imperfect shell.* It was stated in the previous section that in order to predict a non-symmetric collapse of a cylindrical shell by use of the present method, it is necessary to prescribe a certain non-symmetric disturbance. It was also stated that in the elastic buckling of cylinders the analysis will provide a buckling pressure smaller than or equal to the classical buckling load as soon as some type of non-symmetric disturbance is prescribed which allows the critical mode shape to develop.

In the presence of creep, the critical time of a shell corresponds to the critical load in the elastic case, but the value of the critical time is even more dependent on the type and magnitude of the initial imperfection. In particular, the critical time of a cylinder under external pressure approaches infinity if the imperfections tend to zero. The same behavior has been found in the creep buckling theory of columns [15] and [17], which, as was pointed out above, are not imperfection sensitive in elastic buckling. According to [16], the critical time in creep for an idealized H-section column is approximately: $t^* = C \ln (1 + 4/a_0^2)$ where $C$ is a constant and $a_0$ is the initial imperfection amplitude.

In the following examples, the large influence on the creep behavior of the shape and magnitude of an initial imperfection is demonstrated. It may be assumed that a cylinder under radial pressure is sensitive to imperfections of the form:

$$w_0 = \left( \sum_{n=0}^{N} w_{0_n} \cos n\varphi \right) \sin \frac{\pi x}{L}. \tag{28}$$

The results of a few calculations in which this type of imperfection function is included are shown in Fig. 8. The cylinder, $L/R = 2{\cdot}1$ and $R/h = 27$ was loaded by a uniform pressure equal to one quarter of the classical buckling load. Classical buckling theory predicts buckling into 4 waves. The imperfection functions used in the three cases are included in Fig. 8 which gives the amplitudes $\dot{w}_n$ at the midpoint of the shell as functions of time.

In case 1, the coefficients in the Fourier expansion for the imperfection function were all equal. The critical time in creep is according to Fig. 8, 250 sec and buckling occurs into 4 waves. The imperfection function used in case 2 is the same as that of case 1, but the amplitudes have been increased by 25%. A calculation of the elastic collapse load indicated a small difference between the two cases; the critical load was about 75% of the critical load for the perfect cylinder in case 1 and 70% in case 2. However, the critical time is according to Fig. 8, decreased by approximately $\frac{1}{3}$ of that of case 1. The critical time is thus very sensitive to the imperfection level.

In example 3, a different imperfection shape was assumed with a large component in the second harmonic. Also, the amplitude of the 4th harmonic is bigger than that of the previous examples 1 and 2, but the higher harmonic components are small. Although the total amplitude of the imperfection is much larger than those of the previous examples, the critical time is much higher, approximately 1000 sec. This example demonstrates the extreme sensitivity of the creep behavior on the shape of the imperfection.

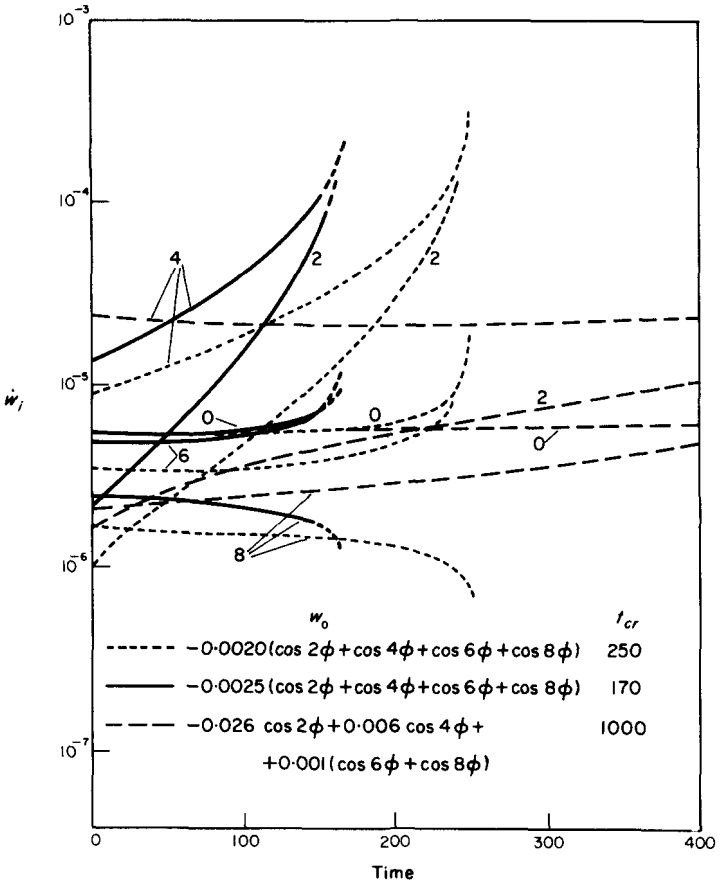


FIG. 8. Load–deflection history of an imperfect shell under uniform radial pressure $R/h = 27, L/R = 2{\cdot}1, n = 3{\cdot}5$.

(c) *Axial compression, perfect shell.* The axisymmetric behavior of a circular cylinder under axial compression has been analyzed by a number of investigators [4–9], which give the axisymmetric collapse mode and the associated critical time. The present program was, for verification, also applied to this case.

Results are shown in Fig. 9 for the axisymmetric creep behavior of a simply supported cylinder with $L/R = 1$, $R/h = 100$ and $E = 5000$. The radial deflection at a time close to the critical is shown in a 3-dimensional plot. The collapse time may be defined as the time at which the maximum radial deflection rate, which appears close to an edge, becomes large. In the present case the critical time is found to be approximately 2·4 hr. This value agrees with the results obtained from the theory for axisymmetric deformation of cylinders presented in [9]. However, it is indicated in [9] that in comparison with experimental results the theory overestimates the critical time. Even for the fairly thick cylinders which do buckle axisymmetrically, theoretical experimental results can differ by a factor of two. It is possible that at least part of this discrepancy is due to initial imperfections.

(d) *Axial compression, imperfect shell.* In the following, the cylinder geometry is the same as in the previous examples used, but imperfections of the form (28) were added. Calculations were carried out for two cases with the Fourier indices 0, 4, 8, . . . , 16 included

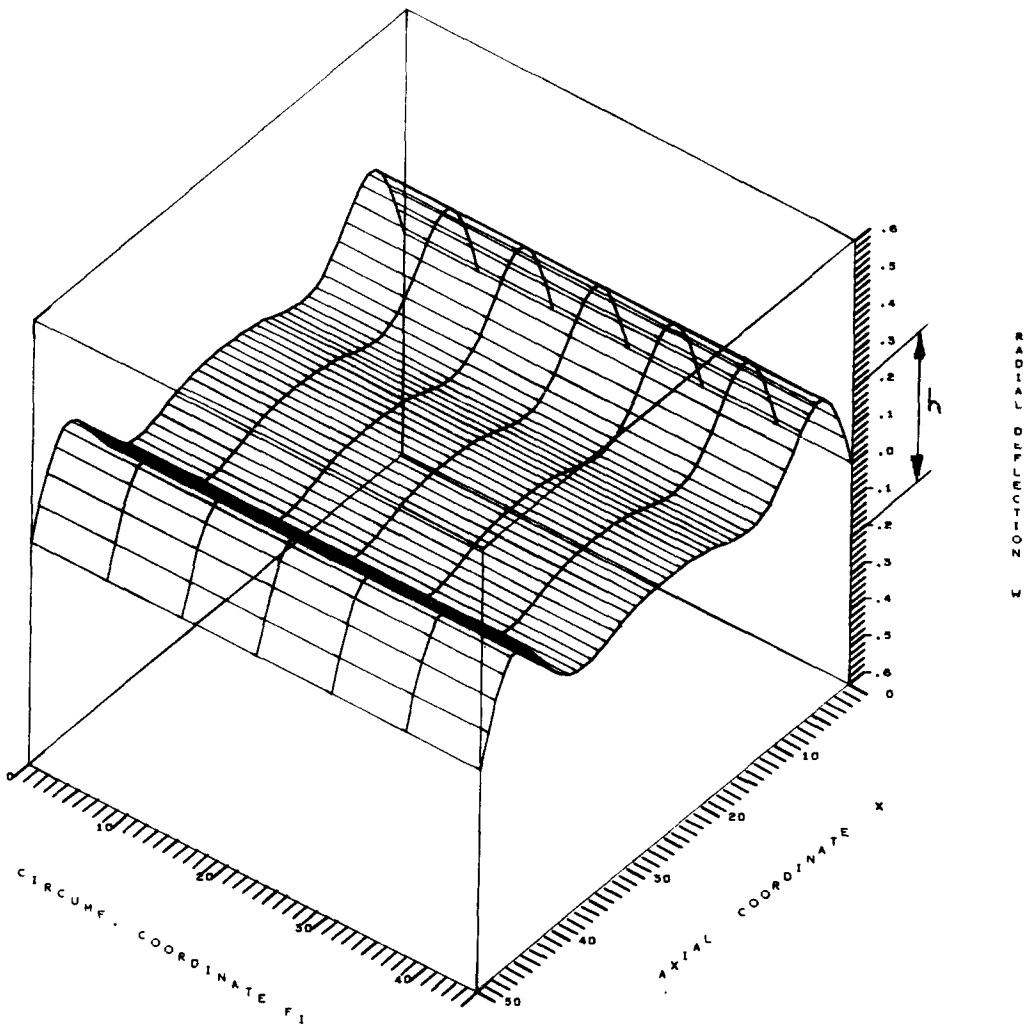


FIG. 9. Radial deflection pattern of a perfect cylinder subjected to axial compression. $R/h = 100$, $L/R = 1$, $E = 5000, n = 5{\cdot}8, t \simeq 2{\cdot}2$ hr.

in the series expansion. The amplitudes of the Fourier terms in the initial imperfection function were all given identical values for each case. Two imperfection levels were investigated, namely $w_{0_n} = -0{\cdot}05$ and $w_{0_n} = -0{\cdot}10$. These initial deformations are shown in Figs. 10a and 10b. The critical times obtained in the analyses were respectively $t_{cr} = 1{\cdot}3$ and 0·6 hr, which should be compared to the time $t_{cr} = 2{\cdot}4$ hr obtained for the perfect shell. It is evident that the presence of an imperfection of the form used (28) may have a drastic influence on the creep behavior of the shell.

The deformation patterns of the shell in the two cases are shown in Fig. 11 at times close to the critical. It is found that the symmetrical deformation mode is fairly well developed in the first case Fig. 11a and a fairly large, nearly symmetric bulge appears close to the edges of the cylinder. In the second case the non-symmetric deformation modes dominate.

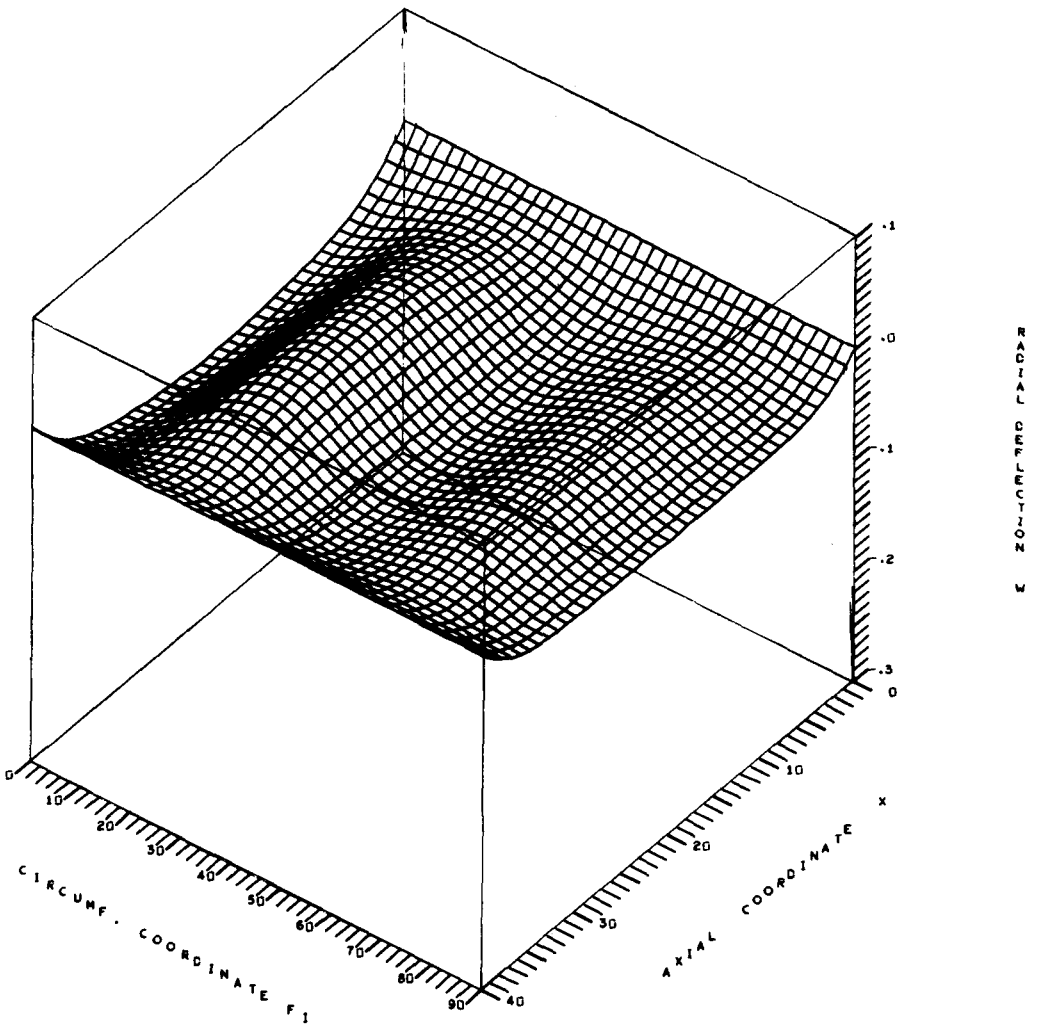


FIG. 10a. Initial imperfections for cylinder with $w_{0_n} = -0{\cdot}05$.

These observations agree qualitatively with those of the experimental investigation of [19]. There it was found that cylinders with approximately the same geometry as those used in the present examples would develop a visible, nearly axisymmetrical bulge close to the edge shortly before collapse occurred. For cylinders with $R/h \gtrsim 40$, a non-symmetric buckling pattern developed. It was, however, also observed in some tests that bifurcation buckling occurred before a visible edge deformation had developed, which, in accordance with the results of the second case above, could have been caused by fairly severe imperfections.

In a last example, a cylinder with $R/h = 100$, $L/R = 1$ and with boundary conditions according to equations (18) was studied. A local imperfection with a length of 20% of the total length and containing the Fourier terms No. 4, 8, 12 and 16 was assumed which implies that this imperfection was repeated over 90° arcs. The amplitudes $w_{0_n}$ were

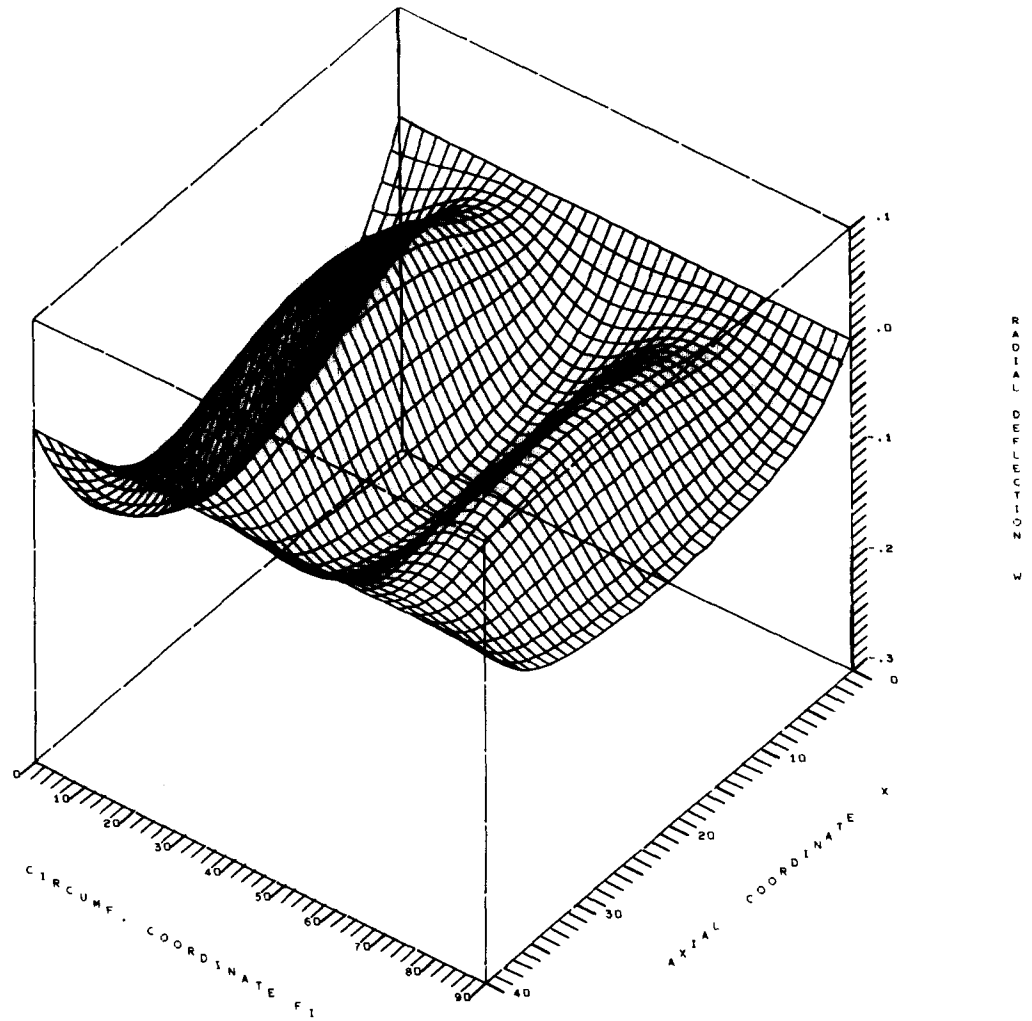


FIG. 10b. Initial imperfections for cylinder with $w_{0_n} = -0{\cdot}10$.

chosen equal to $-0{\cdot}01$. The applied stress was the same as that used in the previous examples, namely $\sigma = 12\,\text{kg/mm}^2$. The critical time obtained for the imperfect cylinder was $t_{cr} \approx 6\,\text{hr}$. The radial deformation immediately before collapse is shown in Fig. 12. As the critical time in this case is higher than that obtained for a perfect cylinder buckling axisymmetrically due to disturbances at the edges it may be concluded that the special type of imperfection assumed is not critical for the cylinder.

## CONCLUDING REMARKS

A theory was presented for the analysis of the creep behavior of circular cylindrical shells under non-uniform loads. As non-symmetric initial imperfections are considered, the analysis is also useful for calculation of the general, nonsymmetric mode of creep collapse of cylinders under uniform loads.

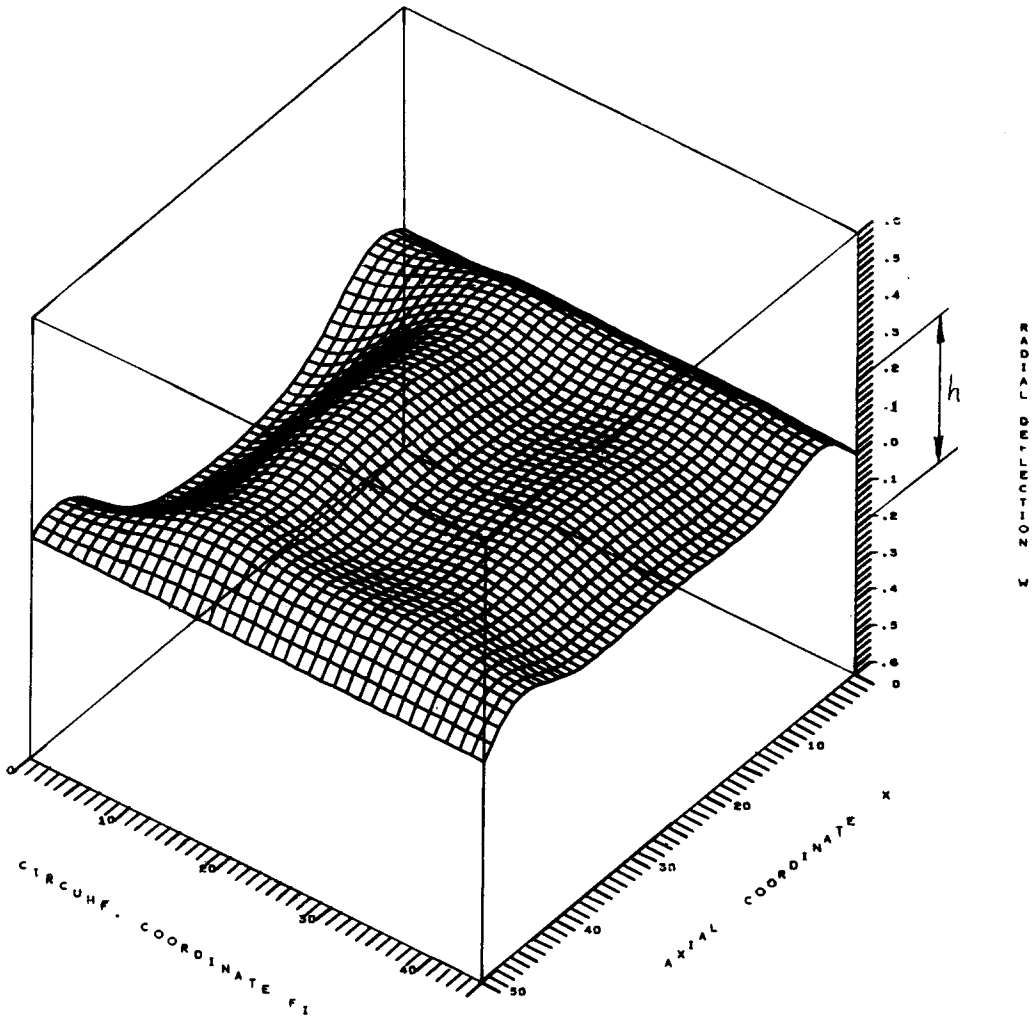


FIG. 11a. Radial deflection pattern of an imperfect cylinder subjected to axial compression. $R/h = 100$, $L/R = 1$, $E = 5000$, $n = 5{\cdot}8$, $w_{0_n} = -0{\cdot}05$, $t \simeq 1{\cdot}2$ hr.

The computer program was verified for the elastic case by comparison with known solutions. It was found that the collapse load predicted by use of the analysis approached the classical buckling load when the initial imperfections were decreased towards zero.

In creep buckling, the critical time was found to depend on the amplitude and shape of the imperfection. In particular, the critical time of a cylinder under axial compression was found to decrease substantially in comparison with that of a perfect shell if initial imperfections of a certain shape and with an amplitude of less than $\frac{1}{4}$ of the wall thickness were introduced. The critical time of a cylinder under radial pressure tends to infinity for infinitesimal imperfections. Hence it appears that a rigorous solution of the problem of creep buckling of cylindrical shells under uniform loads can only be obtained if the initial imperfections are considered.

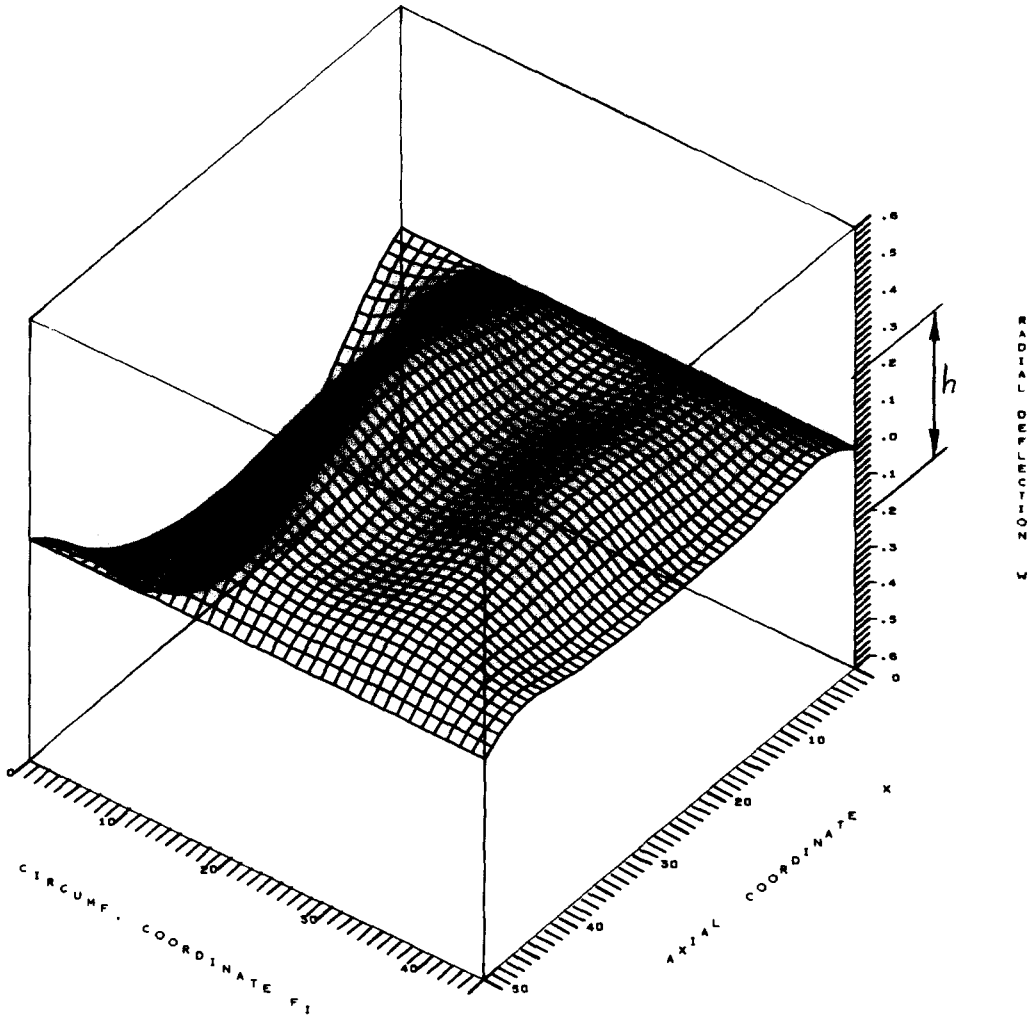


FIG. 11b. Radial deflection pattern of an imperfect cylinder subjected to axial compression. $R/h = 100$, $L/R = 1$, $E = 5000$, $n = 5{\cdot}8$, $w_{0_n} = -0{\cdot}10$, $t \simeq 0{\cdot}55$ hr.

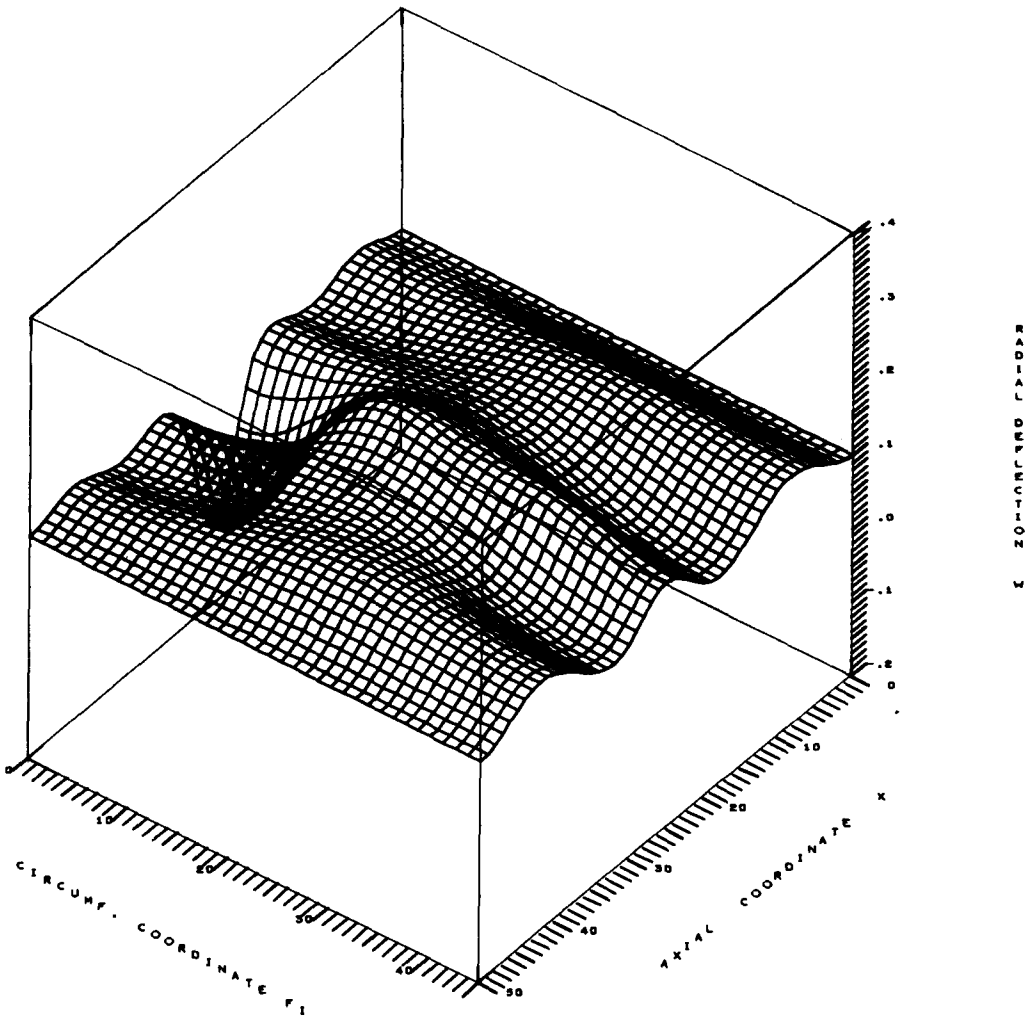


FIG. 12. Radial deflection pattern of a cylinder with a local imperfection. $R/h = 100$, $L/R = 1$ (symmetry conditions), $E = 5000$, $n = 5{\cdot}8$, $t \simeq 5{\cdot}8$ hr.

## REFERENCES

[1] A. KALNINS, Analysis of shells of revolution subjected to symmetrical and non-symmetrical loads, *J. appl. Mech.* **86**, 467–476 (1964).
[2] R. E. BALL, A geometrically non-linear analysis of arbitrarily loaded shells of revolution. NASA CR-909 (1968).
[3] J. A. STRICKLIN, W. E. HAISLER, H. R. MACDOUGALL and F. J. STEBBINS, Non-linear analysis of shells of revolution by the matrix displacement method. Presented at the AIAA 6th Aerospace Sciences Meeting, New York, N.Y., AIAA Paper No. 68-177 (1968).
[4] F. A. COZZARELLI, S. A. PATEL and B. VENKATRAMAN, Creep analysis of circular cylindrical shells. Polytechn. Inst. Bklyn., Dept. Aero. Eng. and Appl. Mech., PIBAL Report No. 685 (1964).
[5] IU. N. RABOTNOV, Axisymmetrical creep problems of circular cylindrical shells. *Prikl. mat. Mekh.* **28**, 1040–1047 (1964). English translation *Appl. Math. Mech.* **28**, 1255–1263 (1964).
[6] E. S. DIAMANT, Axisymmetric creep in cylindrical shells. AIAA Paper No. 66-123 (1966).
[7] B. SCHNEIDER and R. CARLSON, On the creep buckling of axially compressed circular cylindrical shells. Stanford Univ., Dept. Aeron. and Astron., SUDAAR No. 284 (1966).
[8] E. V. PITTNER and N. J. HOFF, Axisymmetric creep deformations of circular cylindrical shells in axial compression. Lockheed Missiles & Space Co., Report No. B-71-67-1. (1967).
[9] L. Å. SAMUELSON, Creep deformation and buckling of a circular cylindrical shell under axial compression and internal pressure. *AIAA J.* 7, 42–49 (1969).
[10] G. GERARD, A unified theory of creep buckling of columns, plates and shells. Presented at the Third International Congress in the Aeronautical Sciences, Stockholm, 1962. Paper No. ICAS-43.
[11] L. Å. SAMUELSON, Creep deformation of a circular cylindrical shell subjected to arbitrary loads. Aero. Res. Inst. Sweden (FFA) Techn. Note No. HU-1111:1 (1966).
[12] W. FLÜGGE, *Stresses in Shells*. Springer (1960).
[13] E. Y. W. TSUI, F. A. BROGAN and P. STERN, Juncture stress fields in multicellular shell structures. Lockheed Missiles & Space Co. Report No. M-77-65-5 (1965).
[14] R. KURE and L. Å. SAMUELSON, USER Instructions—*SALTS* Creep Buckling of a Circular Cylindrical Shell under Axial Compression and Internal Pressure, LMSC Report No. B-70-67-27.
[15] L. Å. SAMUELSON, Non-linear analysis of a circular cylindrical shell under non-uniform external loads and subjected to secondary creep. (USER's Manual for NULACS), Lockheed Missiles & Space Company Report No. B-70-68-16 (1968).
[16] F. K. G. ODQVIST and J. HULT, *Kriechfestigkeit Metallischer Werkstoffe*. Springer (1962).
[17] L. Å. SAMUELSON, Creep buckling of columns, Aero. Res. Inst. Sweden (FFA), Report No. 107 (1967).
[18] R. CARLSON, B. SCHNEIDER and L. BERKE, An experimental study of the creep buckling of circular cylindrical shells under an axially applied compression. Stanford Univ., Dept. Aero & Astron., SUDAER No. 248 (1965).
[19] L. Å SAMUELSON, Experimental investigation of creep buckling of circular cylindrical shells under axial compression and bending. *J. Engng Ind.* **90**, 589–595 (1968).
[20] A. P. KUZNETSOV and N. M. IUNGERMAN, Experimental investigation of shell stability under creep conditions. *Prikl. Mekh. Tekh.* **4**, 128–131 (1965).

## APPENDIX A

*Evaluation of the product of two Fourier series*

In the analysis above, the problem of expressing the product of two Fourier series in terms of one arises. Thus, the coefficients $C_m$ are sought:

$$\sum_{m=0}^{N1} C_m \cos m\varphi = \left(\sum_{n=0}^{NF} a_n \cos n\varphi\right)\left(\sum_{k=0}^{NF} b_k \cos k\varphi\right) \quad \text{or} \tag{A1}$$

$$\sum_{m=0}^{N1} C_m \sin m\varphi = \left(\sum_{n=0}^{NF} a_n \sin n\varphi\right)\left(\sum_{k=0}^{NF} b_k \cos k\varphi\right). \tag{A2}$$

The product may be evaluated according to:

$$\left(\sum_{n=0}^{NF} a_n \begin{Bmatrix}\sin\\ \cos\end{Bmatrix} n\varphi\right)\left(\sum_{k=0}^{NF} b_k \begin{Bmatrix}\sin\\ \cos\end{Bmatrix} n\varphi\right) = \sum_{n=0}^{NF}\sum_{k=0}^{NF} a_n b_k \begin{Bmatrix}\sin\\ \cos\end{Bmatrix} n\varphi \begin{Bmatrix}\sin\\ \cos\end{Bmatrix} k\varphi \tag{A3}$$

where either sin or cos is used.

Now, the well known trigonometry functions

$$\begin{cases} 2\cos A\cos B = \cos(A+B)+\cos(A-B) \\ 2\sin A\sin B = -\cos(A+B)+\cos(A-B) \end{cases} \tag{A4}$$

can be applied, yielding:

$$\sum_{n=0}^{NF}\sum_{k=0}^{NF} a_n b_k \begin{Bmatrix}\sin\\ \cos\end{Bmatrix} n\varphi \begin{Bmatrix}\sin\\ \cos\end{Bmatrix} k\varphi = \frac{1}{2}\sum_{n=0}^{NF}\sum_{k=0}^{NF} \pm a_n b_k(\cos(n+k)\varphi + \cos|n-k|\varphi) = \frac{1}{2}\sum_{l=0}^{2NF} c_l \cos l\varphi . \tag{A5}$$

## APPENDIX B

*Evaluation of the creep terms HC*

The creep terms given by equations (12) have to be developed into Fourier series. As the exponent $m$ is an arbitrary constant it is not possible to do this operation in the same way as for the non-linear terms without much additional labor. Therefore, the Fourier coefficients are calculated numerically in the following way: First evaluate the stresses from:

$$\sigma_{1-4} = \sum_{0}^{NF} \sigma_n \cos nN_p\varphi$$
$$\sigma_{5,6} = \sum_{1}^{NF} \sigma_n \sin nN_p\varphi . \tag{B1}$$

Then, the creep terms of equations (12) are evaluated at a number of equi-distant points $NFIS$ along the circumference. It is assumed that the number of points used is so large that the creep functions may be approximated by straight lines between these points, which is also, in a first approximation, assumed to apply to the trigonometric functions. Then we have

$$H(\varphi_i < \varphi < \varphi_{i+1}) = H_i + \frac{1}{\Delta\varphi}(H_{i+1}-H_i)(\varphi-\varphi_i). \tag{B2}$$

Now, provided the number of circumferential mesh points is sufficiently large, the integrals of equations (25) may be obtained from:

$$\mathbf{F}_0 = \frac{1}{\varphi_{N_p}}\int_0^{\varphi_{N_p}} \mathbf{F}\,d\varphi \simeq \frac{1}{\varphi_{N_p}}\sum_{i=1}^{NFIS-1} \mathbf{F}^i\Delta\varphi. \tag{B3}$$

$$\mathbf{F}_n = \frac{2}{\varphi_{N_p}} \int_0^{\varphi_{N_p}} \mathbf{F} \begin{Bmatrix} \sin nN_p\varphi \\ \cos nN_p\varphi \end{Bmatrix} \mathrm{d}\varphi \simeq \frac{2}{\varphi_{N_p}} \sum_{i=1}^{NFIS-1} \mathbf{F}^i \begin{Bmatrix} \sin nN_p\varphi_i \\ \cos nN_p\varphi_i \end{Bmatrix} \Delta\varphi \tag{B4}$$

according to the trapezoidal integration formula. Advantage has been taken of the fact that $\mathbf{F}^1 = \mathbf{F}^{NFIS}$ due to the assumption of symmetry.

(*Received* 14 *November* 1968; *revised* 18 *April* 1969)

**Абстракт**—Дается метод расчета круглых цилиндрических оболочек, подверженных влиянию неравномерной внешней нагрузки. Уравнения справедливы для умеренно больших перемещений и унитывают второстепенную ползучесть. Учитываются также термические эффекты и начальные неправильности.

Принимая во внимание нелинейные общие уравения, используется итарационный способ численного расчета. Рассматриваются, как известные, нелинейные члены при определенной итерации, полученные раньше в предыдущей итерации. Можно их рассматривать в качестве псевдо нагрузки, прилагаемые в смысле нагрузок к действительным членам нагрузки. Разлагаются переменные зтих линеаризованных диффернциальных уравнений в ряды фурье, используя полярную координату. В результате получается ряд систем обыкновенных дифференциальных уравнений, по одной системе для каждого коэффициента фурье. Ремаются системы уравнений, используя метод конечных разностей. Уравнения ремаются несколько раз для каждого скачка нагрузки или ьремени вплоть до получения сходимостм.

Разработано программу для выислительной машины и проверено, путем сравнения, с известными решениями для упругого выпучивпния оболочек. Указывается теоретическое поведения цилиндра при наличии ползучести для некоторого числа разных условий нагрузки. В особенностси, исследуется реакция оболочки с начальными неправильностями, подверженной влиянию одномерной нагрузки. Для случая внешнего давления, констатируется, что критическое время чрезвычайно чуствительно на неправильность формы. Показывается, что для короткого цилиндра, сжимаемого в осевом направлении, наличие начальных неправильностей сокращает к значительной степени действие ползучести по сравнению с критическим временем, соответствующим осесимметрическому разрушению идеальной оболочки.